Electrochimica Acta 140 (2014) 427–433

Contents lists available at ScienceDirect

Electrochimica Acta

journal homepage: www.elsevier.com/locate/electacta

Comparative degradation of indigo carmine by electrochemical oxidation and advanced oxidation processes

Ricardo E. Palma-Goyes[a], Javier Silva-Agredo[a], Ignacio González[b], Ricardo A. Torres-Palma[a,*]

[a] *Grupo de Remediación Ambiental y Biocatálisis, Universidad de Antioquia UdeA, Medellín, Colombia. A.A 1226, Medellín, Colombia*
[b] *Universidad Autónoma Metropolitana-Iztapalapa, Departamento de Química, Av. San Rafael Atlixco N° 186, C.P 09340, México D.F, México*

ARTICLE INFO

Article history:
Received 6 February 2014
Received in revised form 17 June 2014
Accepted 17 June 2014
Available online 24 June 2014

Keywords:
Dyes
Indigo Carmine
Water treatment
Electrochemical oxidation
photo-Fenton
TiO_2 photocatalysis
Sonochemical degradation

ABSTRACT

The remediation of aqueous effluents containing indigo carmine (IC), a highly toxic indigoid dye used as a textile coloring agent and an additive in pharmaceutical tablets and capsules, was studied using four promising technologies: Ultrasound (US), photo-Fenton (PF), TiO_2 photocatalysis (TiO_2/UV) and electrochemical oxidation with Ti/IrO_2-SnO_2-Sb_2O_5 as anode (EO). The main degradation pathway was determined for each system tested. Additionally, the comparative effects of initial pH and presence of chloride ions was investigated. The results showed that EO of IC was mediated by chloride, whereas IC degradation by TiO_2/UV occurred directly in valence band holes of the catalyst. However, with PF and US systems hydroxyl radicals $^{\bullet}$OH played the main role. In spite of the different degradation pathways, acidic pH increased the performance of all systems. The presence of chloride favored the efficiency of EO, but inhibited the IC removal by PF, as well as the elimination of Chemical Oxygen Demand (COD) by US and TiO_2/UV. The results showed that, under working conditions, EO with Ti/IrO_2-SnO_2-Sb_2O_5 anodes is the best option to treat IC in effluents containing a significant concentration of chloride ions

1. Introduction

Wastewater from textile industries frequently contains significant amounts of non-biodegradable dyes [1]. Most of these dyes are toxic and potentially carcinogenic in nature and their removal from the industrial effluents is a major environmental concern [2].

One of the most widely used dyes in the textile industry is indigo carmine or acid blue 74 (3,3- dioxo-2,2-bis-indolyden-5,5-disulfonic acid disodium salt) (Fig. 1), which is also used as an additive in pharmaceutical tablets and capsules and for medical diagnostic purposes [3]. However, this highly toxic indigoid class of dye is carcinogenic, and can lead to reproductive, developmental, neuronal and acute toxicity and provoke tumors at the site of application [4]. It is also known to cause mild to severe hypertension and have cardiovascular and respiratory effects in patients [5]. Thus, the removal of indigo carmine from water and wastewater is a need of the highest order.

Various technologies have been employed to remove IC from water and wastewater. Physical treatments such as adsorption on chitin and chitosan [6], and on charcoal from extracted residue of coffee beans have been tested [7]. However, these physical systems only transfer the pollutants from the liquid to a solid phase, requiring further treatment and thereby increasing the cost of the process. Other systems, such as incineration, are costly and in most cases can lead to the generation of air pollutants and greenhouse gases [8]. Thus, it is necessary to look for economical and efficient alternative methods for IC degradation.

In the recents years advanced oxidation processes (AOPs) have appeared as interesting alternatives for treating water containing organic pollutants [9–12]. The common denominator of all AOPs is the production and use of hydroxyl radical, which is considered the most powerful oxidizing agent in aqueous phase (E°=2.8 V/SHE, standard hydrogen electrode). Fenton, photo-Fenton system, Photocatalysis, Ultrasound and electrochemical oxidation using BDD are among the most used AOPs.

Some AOPs have been used for IC degradation in water. Vautier et al., 2001[13] studied the degradation of indigo and indigo carmine (64 μM) by TiO_2/UV and achieved a complete mineralization of the dye. Some details on IC degradation mechanism indicated that the main intermediaries formed are carboxylic acids that via photo-Kolbe reaction are the main source of CO_2 evolution. Barka et al., 2008 [14] showed that there is an effect of temperature and pH on IC degradation rate by TiO_2/UV. On the other hand,

---

* Corresponding author. Tel.: +57 4 219 56 00; fax: +57 4 219 56 66.
E-mail addresses: ricardo.torres@udea.edu.co, rtorres@matematicas.udea.edu.co, riantopa@yahoo.com (R.A. Torres-Palma).

http://dx.doi.org/10.1016/j.electacta.2014.06.096

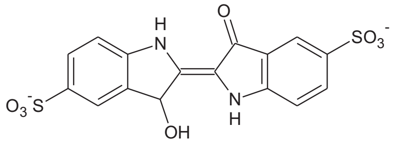

Fig. 1. Chemical structure of indigo carmine dye (IC).

Ammar et al., 2006[15] demonstrated that anodic oxidation by boron-doped diamond (BDD) electrodes can be applied in remediation of wasterwater containing IC (1929 μM, 0.05 M Na_2SO_4). In this study, IC degradation rate was shown to increase significantly with the increase in IC concentration and current density; also, that the pollutant degradation was higher at alkaline pH. T. Makuta et al., 2013 [16] reported IC degradation by Ultrasound (42.88 μM). The variation in the applied potency and the flow and type of dissolved gas affected significantly the dye degradation in water. In a comparative study of different techniques of advanced oxidation, Ureña de Vivanco et al., 2013 [17] studied IC degradation (22.5 μM) by UV/H_2O_2, Photo-Fenton and electrochemical oxidation using BDD anodes, and achieved a total dye removal requiring a different amount of energy for each process.

Flox et al., 2006 [18] studied IC degradation (1929 μM) by electro-Fenton and photo-Electro-Fenton in acid medium (pH 3). A pseudo-first-order kinetics was determined for these systems. The electrochemical oxidation of IC using cylindrical Pb/PbO_2 anodes was performed by El-Ashtoukhy, 2013 [19] who studied the effect of a supporting electrolyte, pH and IC concentration. The use of this system resulted in a total removal of IC and 82% of chemical oxygen demand (COD).

Both EO and AOPs have reported good efficiencies for the treatment of effluents from textile wastewaters. However, each system with its unique characteristics and advantages, offers several ways to generate different oxidizing species, which are also strongly influenced by water composition. Thus, wastewater characteristics may either inhibit or enhance the degrading action of the processes [20,21]. An understanding of the main degradation pathway, as well as of the effect of critical parameters, such as pH and matrix composition, during the treatment is essential to evaluate the applicability of each system. Because blue denim laundry industrial wastewater shows variable chloride concentrations and pH, the main goal of this work is to evaluate the influence of chloride and pH on the degradation of IC dye by photo-Fenton, TiO_2 photocatalysis, high frequency ultrasound and electrochemical oxidation using a DSA anode (Ti/IrO_2-SnO_2-Sb_2O_5). We also propose here the main degradation pathway of each process.

2. Experimental

2.1. Chemicals

Titanium dioxide Degussa P-25 with a surface area of 50 m^2g^{-1} (size ~20-30 nm) was used as provided. IC and hydrogen peroxide (30% for analysis) were purchased from Meyer. Sodium sulfate (Na_2SO_4), sodium chloride (NaCl), potassium iodide (KI), ammonium heptamolybdate ($(NH_4)_6Mo_7O_{24}.4H_2O$), ferrous sulfate heptahydrate (reagent grade) and sodium bicarbonate ($NaHCO_3$) were obtained from Merck. Sulfuric acid and sodium hydroxide, used to adjust the pH as required, were purchased from Sigma Aldrich and Carlo Erba, respectively. A 2 mM stock solution of IC in distilled water was prepared and diluted to 42.88 μM (20 mg L^{-1}) for individual experiments. The selection of dyestuff concentration was based on a suitable pollutant concentration for the analytical test (COD and dye evolution) over a significant timescale (neither too short nor too long).

2.2. Reactor setup

Tests by photo-Fenton (PF), TiO_2 photocatalysis (UV/TiO_2) and electrochemical oxidation were carried out in a cylindrical glass Pyrex compartment of 150 mL of volume. Photo-Fenton and TiO_2 photocatalysis experiments were carried out in an 80-cm^2 camera illuminated from the top with a set of 5 cylindrical Phillips UV lamps (emission maximum at 365 nm), delivering 150 W of total electric power.

In a typical TiO_2 photocatalysis run, 1 g L^{-1} of TiO_2 was added to the reaction mixture and the suspension was left for 2 h in the dark to ensure complete equilibration of pollutant adsorption/desorption on the catalyst surface. After that period of time, the UV lamp was turned on, and this was taken as time zero for the reaction. The reaction set was sampled periodically and filtered with 0.45 μm Millipore filters. During IC degradation by photo-Fenton, iron and hydrogen peroxide concentrations were 5 and 69.1 mg L^{-1} respectively. The iron concentration (5 mg L^{-1}) was established according to Colombian legislation for residual waters (ordinance 1594 of the Colombian Department of Agriculture). It has been reported that during photo-Fenton, optimal hydrogen peroxide concentration is 10 to 25 times the iron concentration [22,23]. Therefore, a H_2O_2/Fe^{2+} ratio of 23 was selected in this work.

The source of ultrasonic irradiation was a piezoelectric disc (diameter 4 cm) fixed on a Pyrex plate (diameter 5 cm) at the bottom of a batch home-made reactor (300 mL). Electrical ultrasonic power was adjustable to 60 W, while the frequency was fixed at 634 kHz. The temperature of the tank was controlled through a cooling jacket at 20 ± 1 °C and displayed by a thermocouple immersed into the solution. Ultrasonic energy dissipated in the reactor (50% of the electrical power input) was estimated by the calorimetric method.

Electrochemical experiments for IC oxidation were carried out in a 150 mL one-compartment electrolytic cell. The anode was a DSA-type electrode (Ti/IrO_2-SnO_2-Sb_2O_5) of 4 cm^2 area, which was in contact with the aqueous solution of the substrate. The current density was 7.5 mA cm^{-2}. The DSA electrode was prepared by the Pechini method according to Pérez et al., 2008 [24]. The cathode was a 10-cm long zirconium spiral. The system was maintained under constant stirring at 150 rpm.

An aqueous solution with 0.05 M sodium chloride (or sodium sulfate) was introduced into the reactors, in order to have a typical concentration of these species as in effluents from the textile industry [25]. As needed, the solutions were made either alkaline by the addition of aqueous NaOH or acidic by adding aqueous H_2SO_4 solutions. Experiments were done at least by duplicate and 2 mL aliquots were periodically sampled for UV visible IC quantification, COD analysis, and oxidant determination.

2.3. Analysis

Quantitative analysis of IC was done by UV visible spectroscopy in a Spectronic UV/Vis Jenway 6320D spectrophotometer set at 611 nm. Evolution of hydrogen peroxide and chlorinated oxidizing species was determined iodometrically: aliquots taken from the reactor were added to a quartz cell containing potassium iodide (0.1 M) and ammonium heptamolybdate (0.01 M). The absorbance was recorded at 350 nm after 2 minutes of reaction. To avoid interferences, absorbance of the dye was also measured at 350 nm, under the same conditions, and the obtained value was taken into account to the quantification of these oxidative species. COD measurements were carried out according to the closed reflux titrimetric method (Standard Methods for the Examination of Water and Wastewater, Method 5520), using a dichromate solution as an oxidizer in a strong acid medium [26]. Test solution was transferred into the dichromate reagent and digested at 150 °C for

2 h. Optical density for color change of the dichromate solution was determined at 420 nm after having completed the calibration of the spectrophotometer.

Cyclic voltammetry experiments were carried out in a single-compartment three-electrode cell using an Autolab PGSTAT 30. The counter electrode was a zirconium spiral, the reference electrode was Ag/AgCl$_{(s)}$/KCl$_{(sat)}$, and the working electrode was the DSA anode described previously. The potentials were applied starting from the open circuit potential (OCP) (0.6 V/SHE) in the potential range (-0.5 to 2.0 V/SHE). The experiments were performed at room temperature under nitrogen atmosphere with 7 mL of solution (1 mM of IC in 0.05 M NaCl).

3. Results and discussion

3.1. Degradation of indigo carmine by AOPs

3.1.1. Sonochemical degradation of indigo carmine

Sonochemical degradation of organic compounds involves the use of ultrasonic waves to generate acoustic cavitation. As a result of this phenomenon, localized hydroxyl radicals from water and oxygen dissociation are generated (Eqs. 1-4) [27].

$$H_2O+)))) \rightarrow H^{\bullet}+{}^{\bullet}OH \tag{1}$$

$$O_2 \rightarrow 2O^{\bullet} \tag{2}$$

$$O^{\bullet}+H_2O \rightarrow 2\bullet OH \tag{3}$$

$$H^{\bullet}+O_2 \rightarrow {}^{\bullet}OH+{}^{\bullet}O \tag{4}$$

The ultrasonic degradation of IC in distilled water is shown in Fig. 2. Under operating conditions (60 W, 20 mg L^{-1} IC, natural pH 5.6) ~50% of initial pollutant is removed in 1 h of treatment. There are three zones in which the degradation of organic compounds can be carried out upon ultrasonic action: inside the cavitation bubble, where pyrolysis is predominant; at the bubble-solution interface, where the degradation occurs via hydroxyl radicals and, in some cases, by pyrolysis; and in the bulk of the solution, in which organic degradation occurs via hydroxyl radical or hydrogen peroxide, mainly coming from $^{\bullet}$OH radical recombination (Eq. 5) [28–30].

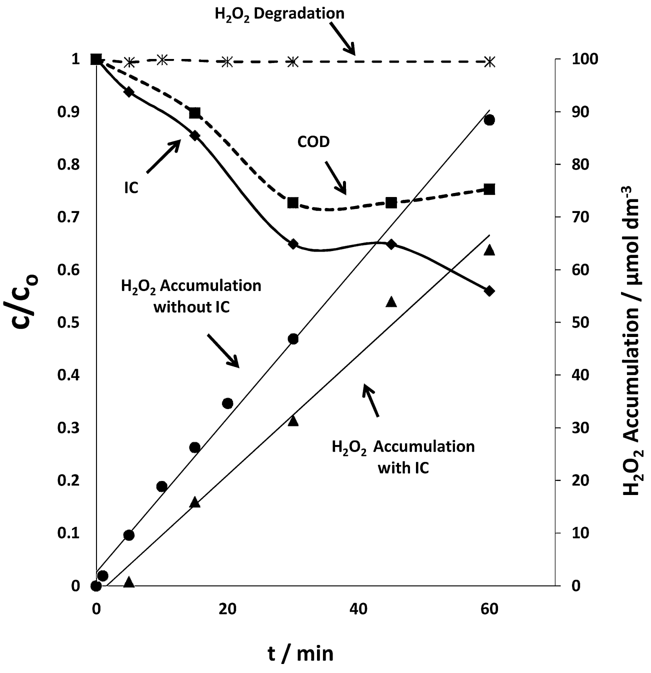

Fig. 2. Evolution of indigo carmine (IC) and COD normalized concentrations during ultrasonic action. The role of H_2O_2 on IC and the H_2O_2 accumulated during the ultrasonic action is also shown. Conditions: IC 20 mg L^{-1}, natural pH 5.6, 60 W and 634 kHz.

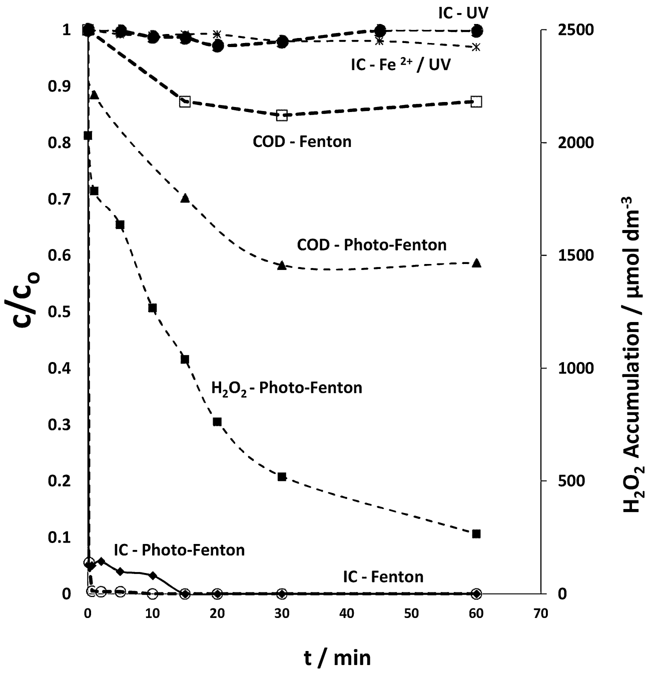

Fig. 3. Evolution of IC and COD normalized concentrations during Fenton and Photo-Fenton degradation processes. The role of UV and UV/Fe^{2+} in the process and the H_2O_2 accumulated during the Photo-Fenton system is also shown. Conditions: 20 mg L^{-1} IC, pH 5.6, 69.1 mg L^{-1} H_2O_2, 5 mg L^{-1} Fe $^{2+}$ and 150 W.

$${}^{\bullet}OH+{}^{\bullet}OH \rightarrow H_2O_2 \tag{5}$$

In order to elucidate the main degradation pathway using ultrasound, the hydrogen peroxide accumulation during water sonication was evaluated in the presence and absence of IC. Fig. 2 also shows that in both cases a linear accumulation of hydrogen peroxide is observed. However, H_2O_2 accumulation is significantly higher in the absence than in the presence of IC. In fact, after 1 h of treatment, H_2O_2 concentration reaches 88 and 64 µmol L^{-1}, in the absence and presence of IC, respectively. A control test (Fig. 2) showed that under working conditions, IC is stable towards oxidation with hydrogen peroxide. Thus, given the low volatility of the IC, the results suggest that the contaminant is degraded mainly by hydroxyl radicals formed during the implosion of gaseous cavities. In fact, a high degradation rate between IC and $^{\bullet}$OH has been reported ($k = 1.8 \times 10^{10}$ M^{-1}s^{-1}) [31]. Fig. 2 also shows that after 1 h, 25% of the initial COD is eliminated. The preceding results indicate that ultrasonic action, via $^{\bullet}$OH radical attack, is able to transform IC into more oxidized by-products.

3.1.2. Photo-Fenton degradation of indigo carmine

Photo-Fenton oxidation of IC was carried out at natural pH (5.6), 69.1 mg L^{-1} (2.03×10^{-3} M) of H_2O_2, 5 mg L^{-1} (9.09×10^{-5} M) of Fe^{2+} and 150 W. Under experimental conditions a rapid decrease of the dye was achieved. In fact, in ~40 seconds the concentration of the dye was below the detection limit (Fig. 3). The role of each component in this reaction (UV, H_2O_2, Fe^{2+}/UV and Fe^{2+}/H_2O_2) was examined in several control experiments (Fig. 3). UV light alone had no effect on IC elimination, even after relatively long irradiation periods (60 min). It demonstrates a marked stability of the dye under UV irradiation. Fig. 3 also shows that Fe^{2+} and light combination does not significantly degrade the pollutant. Thus it follows that neither iron nor light alone, or even the combination of both, affect the concentration of IC in solution. Additionally, the stability of the contaminant towards hydrogen peroxide action was proved and discussed in the previous section (Fig. 2). It is interesting to note that IC elimination by Fenton and photo-Fenton were very fast and quite similar (Fig. 3). Therefore, the results indicate that, under working conditions, the hydroxyl radical is the main oxidizing agent in the photo-Fenton process.

On the other hand, although the removal of the dye is very fast, as shown in Fig. 3, the chemical oxygen demand is not eliminated so easily. Indeed, ~42% of COD is eliminated in 30 min and no further COD diminution is observed in the next 30 min of treatment (1 h). This behavior seems to be related to a huge decrease in hydrogen peroxide concentration after 30 min. Thus, under working conditions, hydrogen peroxide seems to be the limiting reagent for the photo-Fenton process.

Greater efficiencies in the degradation of the contaminant with respect to those achieved by ultrasound, may be explained by the hydrophilic character of the pollutant and the homogeneous character of the Fenton and photo-Fenton systems, which facilitate the contact between the pollutant and the $^\bullet$OH radicals generated in the bulk of the solution.

Finally, even if Fenton and photo-Fenton were quite similar for the removal of the dye, as observed in Fig. 3, efficiencies in the elimination of the COD were significantly different. In the absence of light (Fenton system), only ~15% of the initial COD was removed in 30 min compared with ~42% removal using the photo-Fenton treatment. This indicates that UV light plays a relevant role in the transformation of the degradation intermediates. This is an important aspect because the generated by-products could be more toxic than the initial pollutant and then, the only abatement of IC is not sufficient in the treatment processes.

3.1.3. TiO_2 photocatalytic degradation of indigo carmine

The use of TiO_2/UV system to treat wastewater has been successfully tested in recent years in both lab and pilot scale applications [32]. The degradation of the IC dye upon TiO_2/UV was tested and is shown in Fig. 4. Studies in the dark, indicated that the adsorption-desorption equilibrium of the dye on the catalyst surface was achieved after ~90 min. It was found that ~25% of the initial substrate was adsorbed on the TiO_2 surface (data not shown). Thus, after 2 h of stirring in the dark, the solution was irradiated at 365 nm and 150 W of electrical power; within the first 30 min of irradiation, 92% of the IC was eliminated (Fig. 4). Degradation of contaminants by TiO_2 photocatalysis can be carried out in two ways: by photo-reduction or photo-oxidation at either conduction or valence band, respectively. Fig. 4 also shows that 23% of the initial COD was removed in 1 h of treatment. The significant IC oxidation degree rules out the photo-reduction route as the main IC degradation pathway. On the other hand, during photo-oxidation, the contaminant can be directly oxidized either at the valence band holes (h^+_{BV}), or by hydroxyl radicals, generated from water and hydroxyl ions adsorbed at the holes (Eq. 6-7).

$$TiO_2 + h\nu \rightarrow e^-_{CB} + h^+_{BV} \quad (6)$$

$$(\mathrm{H_2O} \leftrightarrow \mathrm{H^+{+}OH^-})_{ads} + \mathrm{hv}^+_{BV} \rightarrow \mathrm{H^+{+}}^\bullet\mathrm{OH} \quad (7)$$

The photo-generated holes are strong oxidizing agents (2.53 V vs. SHE) and can therefore degrade organic pollutants [33]. In order to identify the main IC oxidation pathway upon the TiO_2/UV system, acetonitrile was used as a reaction medium. In acetonitrile, $^\bullet$OH radicals cannot be formed due to the absence of water or hydroxyl ions in solution. Thus, if IC oxidation occurs via hydroxyl radicals, no degradation of the substrate would be observed when acetonitrile is used as solvent. Fig. 4 shows that the pollutant oxidation is carried out in almost equal proportion in both aqueous and acetonitrile media. This finding demonstrates that, under working conditions, the main initial degradation of the dye by TiO_2/UV system may be occurring via direct oxidation at the hole generated in the valence band. These results are in agreement with previous results, where the initial degradation by TiO_2 photocatalysis was suggested to occur via attack at the central double bond of IC, after pollutant adsorption onto the catalyst surface [13]. This is probably due to the affinity of anionic sulfonic acid groups of the dye (Fig. 1) with the positive holes at the valence band, which promotes adsorption on the catalyst and subsequent oxidation.

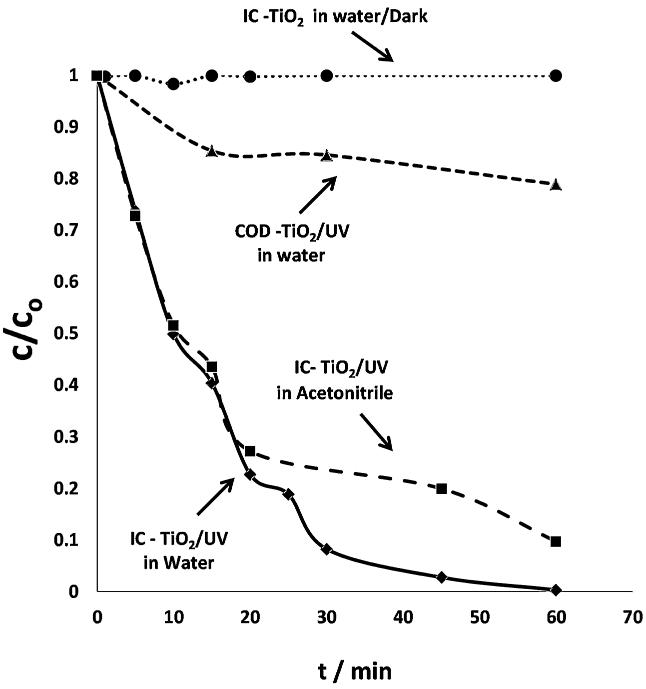

Fig. 4. Evolution of IC and COD normalized concentrations during the TiO_2/UV degradation of indigo carmine in water and acetonitrile as solvents. Conditions: IC 20 mg L^{-1}, natural pH 5.6, 150 W and 1 g L^{-1} of TiO_2.

3.2. Electrochemical degradation of indigo carmine

The presence of salts, commonly associated with wastewaters from the textile industry, permits the use of EO as an alternative for treating these effluents. Therefore, sodium chloride, widely employed in textile industries to fix the dye to the fabric, was selected as supporting electrolyte. The results of electrochemical degradation of IC are shown in Fig. 5. A rapid elimination of the pollutant is achieved in 15 minutes of treatment. In addition, after 1 hour, 42% of COD was removed. Fig. 5 also shows the formation of oxidizing species during the electrochemical treatment. In the absence of pollutant, the accumulation rate of oxidizing agents is 17.9 μmolL^{-1}min^{-1}, while in the presence of the contaminant their accumulation rate is significantly lower (13.0 μmolL^{-1}min^{-1}). These results suggest that chloride present in solution has an active role in the degradation of the substrate. Indeed, it has been reported that in the presence of chloride, DSA anodes promote the formation of chlorine [34]. Hydrolysis of chlorine leads to the formation of HClO and OCl^-. Cl_2, HOCl and OCl^- are species able to oxidize organic matter. Under working conditions (natural pH), HClO is the predominant species and therefore, the main factor responsible for the degradation of IC during the electrochemical treatment. To confirm this hypothesis a new set of experiments on IC degradation by EO were made using sodium sulfate or sodium chloride (0.25 M) as supporting electrolytes (Fig. 6). The IC is practically eliminated in 40 s of treatment in the presence of chloride, whereas when using sulfate only 15% of IC is removed even after 20 min of reaction. The

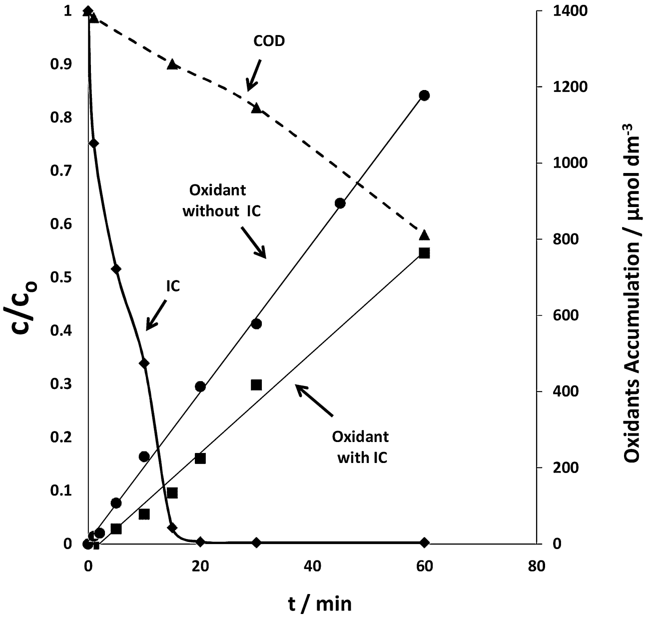

Fig. 5. Evolution of IC and COD normalized concentrations during the electrochemical oxidation (EO) of indigo carmine with a Ti/IrO_2-SnO_2-Sb_2O_5 anode. The oxidant accumulation during the treatment is also shown. Conditions: IC 20 mg L^{-1}, 0.05 M NaCl, pH natural 7.5 mA cm^{-2}.

Fig. 6 inset shows that contrary to what is observed with the use of chloride, no oxidizing species is generated in the case of sulfate. These results highlight the strong positive effect of chloride ions. Therefore, it can be concluded that under working conditions, the electrochemical oxidation of IC is carried out by HClO attack, which is electro-generated from the chloride present in the solution.

3.3. Comparative effect of NaCl on the degradation of indigo carmine by AOPs and electrochemical oxidation

In order to provide a comparative statement of sodium chloride influence on the tested systems (ultrasound, TiO_2/UV, photo-Fenton and electrochemical oxidation), the ratio between the initial degradation rates of the dye in the presence and absence of NaCl, r_{Cl}/r_R, is shown in Fig. 7. The Fig. 7 also shows the ratio of COD, COD_{Cl}/COD_R, within the first hour of treatment in the presence and absence of chloride ions.. As can be observed, when ultrasonic system is used, the presence of sodium chloride does not significantly diminish (only 5%) the sonochemical degradation of IC. This is consistent with the accumulation of hydrogen peroxide during sonication. The H_2O_2 initial rate of accumulation without NaCl was 1.1 µmolL^{-1}min^{-1}; whereas in the presence of chloride ions, the accumulation of hydrogen peroxide was slightly reduced to 1.0 µmolL^{-1}min^{-1} (9% lower - data not shown). Even if chloride ions are recognized to be hydroxyl radical scavengers (Eq. 8) [31], their inhibitory effect on IC elimination is not significant because IC is closer to the cavitation bubbles than the chloride ions.

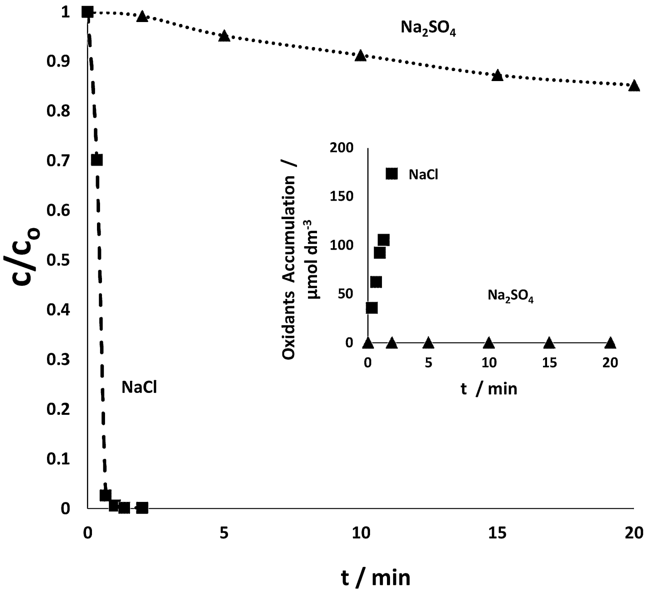

Fig. 6. Evolution of IC normalized concentration during electrochemical degradation (anode: Ti/IrO_2-SnO_2-Sb_2O_5 at 7.5 mA cm^{-2}) of indigo carmine (20 mg L^{-1}) in aqueous solution containing NaCl and Na_2SO_4 as supporting electrolytes (0.25 M). Inset shows the evolution of oxidants during electrolysis.

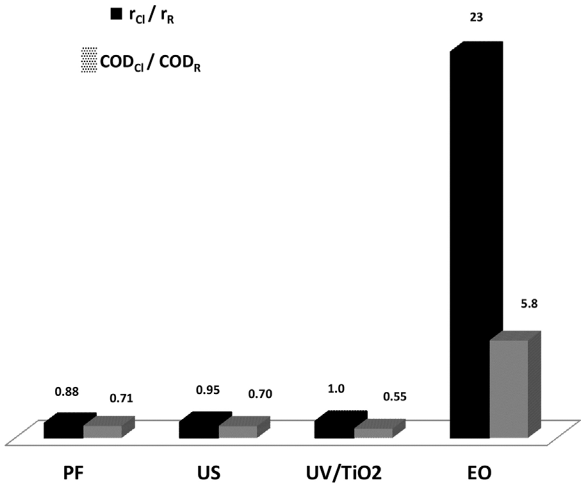

Fig. 7. Effect of chloride ions on the IC degradation by AOPs (PF, Photo-Phenton; US, Ultrasound; UV/TiO_2, Photocatalysis) and electrochemical oxidation (EO). r_{Cl} and r_R are the initial degradation rate of IC in presence and absence of chloride, respectively; while COD_{Cl} and COD_R, represent the chemical oxygen demand in presence and in absence of chloride ions, respectively.

$$Cl^{\bullet} + {}^{\bullet}OH \rightarrow ClOH^{\bullet -} \tag{8}$$

Interestingly, the inhibition of chloride ions on the COD removal was significant (30%). This suggests that IC by-products are more hydrophilic than the initial pollutant, so their removal is more hindered by the presence of chlorides. The formation of by-products more hydrophilic than the initial substrate has been commonly reported when the main degradation pathway upon sonochemical action occurs via hydroxyl radicals [27,35].

The detrimental effect of chloride on the IC removal by photo-Fenton was more evident than the one observed using ultrasound. In the presence of chloride, 16% inhibition was found for IC elimination, while inhibition on COD was 29% (Fig. 7). In addition to the scavenger effect on hydroxyl radicals, chloride anions can form complexes with Fe^{2+}/Fe^{3+} ions (Eq. 9-11), thereby diminishing the concentration of free iron ions, which are necessary for photo-Fenton mechanism [36].

$$Fe^{2+} + Cl^- \leftrightarrow FeCl^+ \tag{9}$$

$$Fe^{3+} + Cl^- \leftrightarrow FeCl^{2+} \tag{10}$$

$$Fe^{3+} + 2Cl^- \leftrightarrow FeCl_2^+ \tag{11}$$

Concerning TiO_2 photocatalysis, section 3.1.3 shows that the degradation of IC by UV/TiO_2 is carried out directly at the holes generated in the valence band and not by hydroxyl radicals, for which reason, the negligible effect of chloride ions on the IC elimination is expected (Fig. 7). However the Fig. 7 also shows a strong inhibition (45%) on the COD parameter. Huge differences found in the IC and COD removals due to the effect of chloride suggest that the main degradation route of the generated IC by-products occurs via hydroxyl radicals.

Both the electrochemical elimination and oxidation of IC are by far favored in the presence of chloride. Taking as reference the rate observed when employing sodium sulfate as electrolyte, the removal and oxidation of the dye increased ~20 and ~6 times, respectively, when chloride was used. This behavior is explained by the high catalityc activity of the anode to transform chloride ions into oxidizing chlorinated species (Eq. 8-10). Thus, the results indicate that, among the systems tested, electrochemical oxidation using DSA anodes is probably the most suitable process to treat wastewaters containing high chloride concentrations.

3.4. *Comparative effect of Initial pH on the degradation of indigo carmine by AOPs and Electrochemical Oxidation*

The pH is a parameter of great interest in wastewater treatments because it can influence both the chemical structure of the contaminant and the reactivity of the process. In addition, it has been reported that textile wastewater shows high pH variability. In order to evaluate the effect of the pH, different solutions of the pollutant at initial pH 2, natural pH (5.6) and pH 10 were evaluated for each one of the tested systems. IC has a p*K*a of 12.6 [15], so it can be anticipated that in the range of all pH used, the IC structure remains unchanged. Control experiments (data not shown) confirmed the stability of the dye at the three pH values selected. The tests were carried out in the presence of chloride to perform studies under conditions closer to those found in real textile wastewater.

Fig. 8 shows, for all of the systems, the ratio between the initial degradation rates under acidic or basic pH related to the initial rate at natural pH. Some interesting differences among the degradation systems were observed. Degradation efficiency by ultrasound is two times higher at acid pH compared to that performed at pH 10 or natural pH. As indicated, due to its hydrophilic character, IC is mainly degraded in the bulk of the solution. Chloride ions, present in the solution, can also react with hydroxyl radicals (Eq. 8). At acidic pH, the following reactions, leading to the formation of $Cl_2^{\bullet -}$ (E^0 redox = 2.20 V vs. SHE) are favored [37]:

$$ClOH^{\bullet -} + H^+ \leftrightarrow Cl^{\bullet} + H_2O \tag{12}$$

$$Cl^{\bullet} + Cl^- \leftrightarrow Cl_2^{\bullet -} \tag{13}$$

Even if the $Cl_2^{\bullet -}$ radical has a lower oxidative power than the $^{\bullet}OH$ radical, it has a longer lifetime, which allows a greater probability of reaction with the contaminant and as a result, enhances the IC degradation.

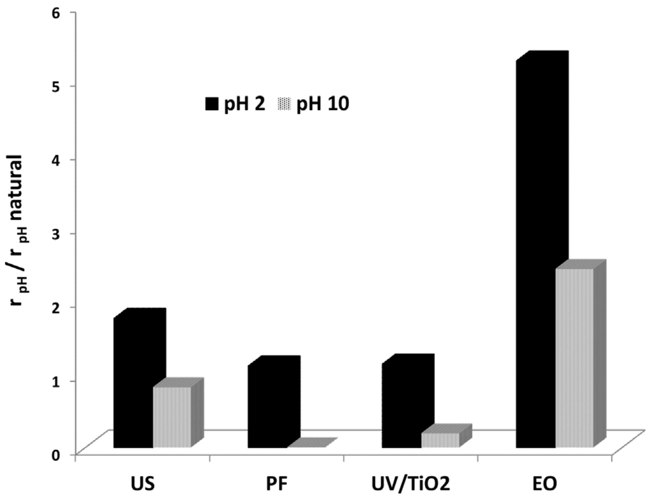

Fig. 8. Effect of pH on the IC degradation by AOPs (PF, Photo-Phenton; US, Ultrasound; UV/TiO_2, Photocatalysis) and electrochemical oxidation (EO). r_{pH}, initial degradation at initial pH of 2 or 10; $r_{pH\ natural}$, initial degradation rate at natural pH (5.6).

During electrochemical treatment, 100% of IC was removed, in all cases, within 15 minutes of treatment (data not shown). However, the initial degradation rate was higher at extreme pH values (2 and 10), Fig. 8, obtaining a greater rate at pH 2 (~5 times higher than at natural pH). The best performance observed at pH 2 is associated with the favorable oxidation of chloride at this pH value (See Supplementary Materials, Fig. SM 1).

The degradation by photo-Fenton also showed a marked dependence on the pH (Fig. 8). In this case, the IC degradation at pH 2 is slightly superior to that found at natural pH (5.6). Although it is well know that the optimum pH for Fenton and photo-Fenton systems is ~3 [38], the results at natural pH are quite good compared to those obtained at acidic pH. These results confirm that this technique is also efficient at circumneutral pH, as has been recently reported for the degradation of several pollutants [11,39]. On the other hand, experiments at pH 10 were strongly hampered. The latter is due to the precipitation of iron ions at basic pH values [40].

Photocatalysis with TiO_2 showed to be quite similar at pH 2 and natural pH (degradation rate ratio was 1.1, whereas at pH 10 the initial degradation rate decreased considerably (Fig. 8). Titanium dioxide is an amphoteric substance, with variable isoelectric point depending on the method of synthesis. In the present work, the TiO_2 used was Degussa P25 (70% anatase, 30% rutile), which reaches its isoelectric point at pH ~6.5. Thus, the pH of solution is expected to affect the activity of TiO_2 including the particle charge, size of aggregates, form and positions of the valence, conduction bands, etc. [41,42]. The TiO_2 particles are positively charged below pH <6.5, while at pH >6.5 the catalyst particles acquire a negative charge (Eq. 14-15). When photocatalytic treatment with TiO_2 is performed at pH 2, the protonated form of the catalyst predominates. Under such conditions, the charge of TiO_2 is opposite to that of IC. Therefore, and due to the electrostatic attraction between IC and TiO_2 particles, the absorption of the pollutant and its degradation is greater [13]. At pH 10, both catalyst and pollutant are charged negatively and then, because of the repulsion between them, lower rates of degradation are obtained (Fig. 8).

$$TiOH + H^+ \leftrightarrow TiOH_2^+ \quad pH < 6.5 \tag{14}$$

$$TiOH + OH^- \leftrightarrow TiO^- + H_2O \quad pH > 6.5 \tag{15}$$

4. Conclusions

The results presented in this work show interesting similarities and differences between AOPs and electrochemical oxidation for IC degradation in water. The main route of oxidation for ultrasound and photo-Fenton was shown to occur via hydroxyl radicals, while TiO_2 photo-catalysis degradation occurred by direct oxidation at the holes generated in the valence band. The results of electrochemical oxidation indicated that indirect degradation occurred by action of chlorinated oxidative species, mainly HClO, electrogenerated at the electrode surface due to the oxidation of chloride ion in solution. Under working conditions, photo-Fenton and electrochemical oxidation were shown to achieve the degradation of contaminant in a relatively short period of time.

The presence of chlorides in the matrix affected differently the evaluated processes. This effect arises from the distinctive mechanisms or degradation pathways presented in each case. Therefore, the presence of these ions was negative for processes in which the oxidation occurred via hydroxyl radical in the bulk of the solution. The most notorious inhibition effect of chloride ions occurred during the IC degradation by photo-Fenton, as well as during the elimination of IC by-products (COD removal) by ultrasound and TiO_2 photocatalysis. In turn, the electrochemical oxidation with Ti/IrO_2-SnO_2-Sb_2O_5 anode, a technique that requires the presence of a conductive medium was, as indicated, favored by chloride ions.

The pH directly affected the treatment systems in multiples ways (e.g. type and concentration of oxidants generated, iron speciation, titanium dioxide structure, etc.), but not the chemical structure of the contaminant. Acidic pH promotes the formation of oxidizing species during electrochemical and ultrasound systems; in photo-catalysis, however, its influence is linked to the TiO_2 surface charge, whose positive charge in acidic media favors the adsorption and subsequent degradation of the anionic pollutant.

Acknowledgements

The authors wish to thank the Swiss National Science Foundation for financial support through the program “Swiss Programme for Research on Global Issues for Development” Project No IZ01Z0_146919 and to ENLAZAMUNDOS for financial support to Mr. Ricardo E. Palma-Goyes.

Appendix A. Supplementary data

Supplementary data associated with this article can be found, in the online version, at http://dx.doi.org/10.1016/j.electacta.2014.06.096.

References

[1] S. Alahiane, S. Qourzal, M. El Ouardi, M. Belmouden, A. Assabbane, Y. Ait-Ichou, Adsorption and photocatalytic degradation of indigo carmine dye in aqueous solutions using $TiO_2/UV/O_2$, J. Mater. Environ. Sci. 4 (2013) 239.

[2] M.A. Rauf, S. Salman Ashraf, Fundamental principles and application of heterogeneous photocatalytic degradation of dyes in solution, Chem. Eng. J. 151 (2009) 10.

[3] U.R. Lakshmi, V.Ch. Srivastava, I.D. Mall, D.H. Lataye, Rice husk ash as an effective adsorbent: Evaluation of adsorptive characteristics for Indigo Carmine dye, J. Environ. Manage. 90 (2009) 710.

[4] C.L. Jenkins, Textile dyes are potential hazards, Arch. Environ. Health 40 (1978) 7.

[5] D.L. Jeffords, P.H. Lance, W.C. Dewolf, Severe hypertensive reaction to indigo carmine, Urology 9 (1977) 180.

[6] A.G.S. Prado, J.D. Torres, E.A. Faria, S.C.L. Dias, Comparative adsorption studies of indigo carmine dye on chitin and chitosan, J. Colloid Interface Sci. 277 (2004) 43.

[7] T. Nakamura, M. Hirata, N. Kawasaki, S. Tanada, T. Tamura, Y. Nakahori, Decolorization of indigo carmine by charcoal from extracted residue of coffee beans, J. Environ. Sci. Health A 38 (2003) 555.

[8] Kapałka A., Foti G., Ch. Comniellis, Basic Principles of the Electrochemical Mineralization of Organic Pollutants for Wastewater Treatment, In: Ch. Comniellis, G., Chen, Electrochemistry for the Environment, 1, springer, New York, 2010, 1.

[9] P. Liu, H. Zhanga, Y. Feng, F. Yang, J. Zhang, Removal of trace antibiotics from wastewater: A systematic study of nanofiltration combined with ozone-based advanced oxidation processes, Chem. Eng. J. 240 (2014) 211.

[10] Y. Juang, E. Nurhayati, Ch. Huang, J.R. Pan, S. Huang, A hybrid electrochemical advanced oxidation/microfiltration system using BDD/Ti anode for acid yellow 36 dye wastewater treatment, Sep. Purif. Technol. 120 (2013) 289.

[11] N. De la Cruz, L. Esquius, D. Grandjean, A. Magnet, A. Tungler, L.F. de Alencastro, C. Pulgarín, Degradation of emergent contaminants by UV, UV/H_2O_2 and neutral photo-Fenton at pilot scale in a domestic wastewater treatment plant, Water Res. 47 (2013) 5836.

[12] L. Prieto-Rodríguez, D. Spasiano, I. Oller, I. Fernández-Calderero, A. Agüera, S. Malato, Solar photo-Fenton optimization for the treatment of MWTP effluents containing emerging contaminants, Catal. Today 209 (2013) 188.

[13] M. Vautier, C. Guillard, J.M. Herrmann, Photocatalytic Degradation of Dyes in Water: Case Study of Indigo and of Indigo Carmine, Journal of Catalysis 201 (2001) 46.

[14] N. Barka, A. Assabbane, A. Nounah, Y. Ait Ichou, Photocatalytic degradation of indigo Carmine in aqueous solution by TiO2-coated non-woven fibres, J. Hazard. Mater. 152 (2008) 1054.

[15] S. Ammar, R. Abdelhedi, C. Flox, C. Arias, E. Brillas, Electrochemical degradation of the dye indigo carmine at boron-doped diamond anode for wastewaters remediation, Environ. Chem. Lett. 4 (2006) 229.

[16] T. Makuta, Y. Aizawa, R. Suzuki, Sonochemical reaction with microbubbles generated by hollow ultrasonic horn, Ultrason. Sonochem. 20 (2013) 997.

[17] M. Ureña de Vivanco, M. Rajab, C. Heim, T. Letzel, B. Helmreich, Setup and Energetic Considerations for Three Advanced Oxidation Reactors Treating Organic Compounds, Chem. Eng. Technol. 36 (2013) 355.

[18] C. Flox, S. Ammar, C. Arias, E. Brillas, A.V. Vargas-Zavala, R. Abdelhedi, Electro-Fenton and photoelectron-Fenton degradation of indigo carmine in acidic aqueous medium, Appl. Catal. B: Environ. 67 (2006) 93.

[19] E.S.Z. El-Ashtoukhy, Removal of indigo carmine dye from synthetic wastewater by electrochemical oxidation in a new cell with horizontally oriented electrodes, Int. J. Electrochem. Sci. 8 (2013) 846.

[20] A. Aleboyeh, M.B. Kasiri, H. Aleboyeh, Influence of dyeing auxiliaries on AB74 dye degradation by UV/H_2O_2 process, J. Environ. Manage. 113 (2012) 426.

[21] C. Pétrier, R. Torres-Palma, E. Combet, G. Sarantakos, S. Baupa, C. Pulgarin, Enhanced sonochemical degradation of bisphenol-A by bicarbonate ions, Ultrason. Sonochem. 17 (2010) 111.

[22] J. Beltran-Heredia, J. Torregosa, J.R. Dominguez, J.A. Peres, comparation of the degradation of p-hydroxibenzoic acid in aqueous solution by several oxidation process, Chemosphere 42 (2001) 351.

[23] S.M. Kim, S.U. Geissen, A. Volgelpohl, Landfill leachate treatment by a photoassisted fenton reaction, Water Sci. and Tecnhol. 35 (1997) 239.

[24] M.R. Pérez, M.T. Oropeza, I. González, J.L. Nava, O. López, I. Gradilla, Preparation and evaluation of electrocatalysts to generate oxygen bubbles for the electroflotation process, ECS Transactions 15 (2008) 51.

[25] F.A. Rodríguez, M.N. Mateo, J.M. Aceves, E.P. Rivero, I. González, Electrochemical oxidation of bio-refractory dye in a simulated textile industry effluent using DSA electrodes in a filter-press type FM01-LC reactor, Environ. Technol. 34 (2013) 573.

[26] A.D. Eaton, L.S., Clesceri, E.W., Rice, A.E., Greenberg, M.A Franson, 2005, Standard Methods for the Examination of Water and Wastewater Twenty-one Edition. Method 5520.

[27] R.A. Torres, R. Mosteo, Ch. Pétrier, C. Pulgarin, Experimental design approach to the optimization of ultrasonic degradation of alachlor and enhancement of treated water biodegradability, Ultrason. Sonochem. 16 (2009) 425.

[28] Y. Adewuyi, Sonochemistry in environmental remediation 1: Combinative and hybrid sonophotochemical oxidation processes for the treatment of pollutants in water, Environ. Sci. Technol. 39 (2005) 3409.

[29] N. Ince, G. Tezcanli, R. Belen, I. Apikyan, Ultrasound as a catalyzer of aqueous reaction systems: the state of the art and environmental applications, Appl. Catal. B-Environ. 29 (2001) 167.

[30] L. Thompson, L. Doraiswamy, Sonochemistry: science and engineering, Ind. Eng. Chem. Res. 38 (1999) 1215.

[31] H. Liao, D. Stenman, M. Jonsson, Study of Indigo carmine as radical probe in photocatalysis, J. Photochem. Photobiol. A: Chemistry 202 (2009) 86.

[32] B. Lopez-Alvarez, R.A. Torres-Palma, G. Peñuela, Solar photocatalitycal treatment of carbofuran at lab and pilot scale: Effect of classical parameters, evaluation of the toxicity and analysis of organic by-products, J. Hazard. Mater. 191 (2011) 196.

[33] S. Ahmed, M.G. Rasul, W.N. Martens, R. Brown, M.A. Hashib, Heterogeneous photocatalytic degradation of phenols in wastewater: A review on current status and developments, Desalination 261 (2010) 3.

[34] G. Chen, Electochemical technologies in wastewater treatment, Sep. Purif. Technol. 38 (2004) 11.

[35] F. Guzman-Duque, C. Pétrier, C. Pulgarin, G. Peñuela, R.A. Torres-Palma, Effect of sonochemical parameters and inorganic ions during the sonochemical degradation of crystal violet in water, Ultrason. Sonochem. 18 (2011) 440.

[36] S.L. Orozco, E.R. Bandala, C.A. Bulnes, B. Serrano, R.S. Parra, I.H. Perez, effect of Iron Salt on The Color Removal of Water Containing the Azo-Dye Reactive Blue Using Photo-assisted $Fe(II)/H_2O_2$ and $Fe(III)/H_2O_2$ Systems, J. Photochem. Photobiol. A: Chem. 198 (2008) 144.

[37] J. Kiwi, A. Lopez, V. Nadtochenko, Mechanism and kinetic of the OH-radical intervention during fenton Oxidation in the presence of a significant amount of radical scavenger (Cl^-), Environ. Sci. Technol. 34 (11) (2000) 2162.

[38] B. Lopez-Alvarez, R.A. Torres-Palma, F. Ferraro, G. Peñuela, Solar photo-Fenton treatment of carbofuran: Analysis of mineralization, toxicity, and organic by-products, J. Environ. Sci. Health Part A47 (2012) 2141.

[39] I. Carra, S. Malato, M. Jiménez, M.I. Maldonado, J.A. Sánchez Pérez, Microcontaminant removal by solar photo-Fenton at natural pH run with sequential and continuous iron additions, Chem. Eng. J. 235 (2014) 132.

[40] J. Pignatello, Advanced Oxidation Processes for Organic Contaminant Destruction Based on the Fenton Reaction and Related Chemistry, Crit Rev in Environ. Sci. Tecnhol. 36 (2006) 1.

[41] T. Sauer, G. Neto, H. Jose, R. Moreira, Kinetics of photocatalytic degradation of reactive dyes in a TiO2 slurry reactor, J. Photochem. Photobiol. A 149 (2002) 147.

[42] B. Neppolian, M. Shankar, V. Murugesan, Semiconductor assisted photodegradation of textile dye, J. Sci. Ind. Res. 61 (2002) 224.